Hindawi
International Journal of Corrosion
Volume 2022, Article ID 4301767, 10 pages
https://doi.org/10.1155/2022/4301767

Research Article

Investigation of Initial Atmospheric Corrosion of Carbon and Weathering Steels Exposed to Urban Atmospheres in Myanmar

Wint Thandar,[1] **Yu Yu Kyi Win**,[2] **Thinzar Khaing**,[3] **Yasuo Suzuki**,[4] **Kunitomo Sugiura**,[5] **and Itaru Nishizaki**[6]

[1]*Department of Civil and Earth Engineering, Kyoto University, 615-8540, Japan*
[2]*Engineering Department, Yangon Region Development Committee, 11182, Myanmar*
[3]*Department of Civil Engineering, Yangon Technological University, 11101, Myanmar*
[4]*Department of Civil Design and Engineering, Toyama University, 930-8555, Japan*
[5]*Department of Civil and Earth Resources Eng., Kyoto University, 930-8555, Japan*
[6]*Innovative Materials and Resources Research Centre, PWRI, 305-8615, Japan*

Correspondence should be addressed to Wint Thandar; wint.thandar.3y@kyoto-u.ac.jp

Received 10 February 2022; Revised 3 March 2022; Accepted 7 March 2022; Published 5 April 2022

Academic Editor: Michael J. Schütze

Copyright © 2022 Wint Thandar et al. This is an open access article distributed under the Creative Commons Attribution License, which permits unrestricted use, distribution, and reproduction in any medium, provided the original work is properly cited.

This research is aimed at studying the corrosion rates of carbon and weathering steels due to exposure at three urban exposure sites and the characteristics of corrosion products of carbon steel in Yangon, Myanmar. The ISO 9223 standard was used to classify the corrosion aggressiveness of the atmosphere. There is a high level of time of wetness (TOW) class which is τ_4 in the south and τ_3 in the central part of Myanmar. At the recent exposure sites in Myanmar, the atmospheric impurities are low, so the corrosion rates of carbon and weathering steels are mainly governed by TOW. The corrosion rates of test sites fall into the ISO C2 category. It appears that corrosion kinetics fit the power model well, since the correlation coefficient is high. Various morphologies of corrosion products including globular, flowery, and sandy lepidocrocite emerged in the early stage of exposure. The longer TOW conditions resulted in the formation of lepidocrocite and goethite. The growth of goethite products on carbon steel was discovered after nine months of exposure.

1. Introduction

Myanmar is situated in a tropical zone; thus, the atmospheric conditions are high in temperature and humidity through a year which causes a long time of wetness (TOW). Moreover, a heavy rainfall over 200 inches (5080 mm) is measured during the monsoon season, especially in the coastal area. In addition, the country possesses a long coastal line which is about 2,300 km, and high chloride concentration in coastal areas is discovered due to the air with high airborne salinity coming in from the Bay of Bengal. Moreover, Myanmar is a developing country which means air pollution is growing up with the development of industrial activities nowadays. These facts affect in significant degradation of materials by atmospheric corrosion.

The study of atmospheric corrosion in Myanmar was initiated in 2014 and Thandar et al. investigated the link between outdoor and accelerated corrosion of weathering steel [1]. However, the implementation of atmosphere aggressiveness and characterization of rust layer by exposure in different urban atmospheres in Myanmar have not been performed yet. The aggressiveness of the atmospheric constituents can be assessed by measuring climatic and pollution factors or by determining the corrosion rates of exposed metals. Corvo et al. detected a significant difference in aggresivity among climatic seasons at the place with a high salinity in tropical climates [2]. Atmospheric corrosion processes have been reviewed and analyzed in detail, and also, several mathematical models have been developed for prediction the corrosion damage of metals in the

atmosphere [3]. However, these developed mathematical models are proposed to explain atmospheric corrosion at a particular region, and these cannot be extrapolated to the other places because the number of variables that is considered by the models is much reduced in comparison with the great number of variables that really influence on atmospheric corrosion process [4].

The formation of corrosion products on metal surfaces depends on the presence of surface contamination and moisture, either in the form of rain, dew, condensation, or high humidity. Different types of corrosive environments are classified by the content of atmospheric aggressive agents (named sulfur dioxide SO_2 and chloride CL^-) [5]. Moreover, the types of atmosphere (rural vs. coastal) drives the kinetics of corrosion and consequently the corrosion products. The kinetics of atmospheric corrosion sometimes does not correspond to one parameter, despite the fact that it is affected by a combination of influenced parameters. A higher amount of wet deposition brings more sea salt near the shore causing higher chloride deposition rate. The significance of higher wet deposition amount's effect on CL^- deposition in Thailand is reported by Wanida et al. [6]. The authors discovered that higher chloride deposition occurred at the test site with more rainfall than at the test site with low rainfall. Also, taking into consideration salt dissolving in the rainfall, it is calculated that CL^- deposition is higher at higher TOW site. In the study of corrosion of carbon steel in Vietnam during the period of 1995-2005, the corrosion of carbon steel is mostly affected by TOW [7]. The major construction material in Myanmar recently is carbon steel due to its relatively low cost and excellent mechanical properties. Due to widespread use of carbon steel in the country, it is desirable to study the atmospheric corrosion behaviors of this steel.

Atmospheric corrosion of steels is strongly dependent on the nature of oxide or rust layer on the steel surfaces. Thus, the characteristic of rust layer is expected to understand certain beneficial effects of corrosion process of steel in the corresponding environment [8]. Corrosion of carbon steel is composed of various oxides such oxyhydroxides, hydrated oxides, miscellaneous crystalline, and other elements resulting from the reaction of iron (Fe) with its surroundings such as the atmosphere [9]. Many researchers studied the corrosion products of atmospheric corrosion by X-ray diffraction (XRD) and Raman spectroscopy. According to their findings, corrosion products formed on the early period of exposure are usually lepidocrocite and later transformed into goethite [10]. The environmental condition is a parameter that affects the structure and size of the corrosion products. It was found that the oxide layer at the chloride enrich environment was irregular and cracked. The oxide layer is characterized by akaganeite, which occurs at chloride-rich environments [11]. The transformation of the oxide layer from lepidocrocite into goethite through prolonged exposure time was observed on the surface of carbon steel exposed in Banda Aceh's atmosphere in Indonesia [12]. The chemical composition of metal significantly affects the rust layer [13]. Hence, the property corrosion products play a role in determining the kinetics of the corrosion reaction on specific material.

In this article, the results of a recent study on atmospheric corrosion over 3 years are discussed at three urban exposure sites. The corrosion rate and characteristics of corrosion products of steel produced in Myanmar have been studied. Depending on how much weight is lost, corrosion rate was calculated. Time of wetness and the level of pollutants, namely, SO_2 and chlorides, were determined in order to establish the aggressiveness of atmospheres. Morphological features of the rust layer were identified with exposure time for further examination of the interplay between corrosion products, environmental factors, and corrosion kinetics in the local areas, in Myanmar.

2. Experimental Procedure

The experimental setup for the measurement of corrosion rate and environmental parameters is similar for all test stations. Specimens were exposed outdoors on a metal rack which was designed by ISO 8565 [14] to allow specimens to be exposed at a 45° angle from horizontal. The climatic parameters which influence atmospheric corrosion; temperature, relative humidity, sulfur dioxide, and airborne salt concentration were measured at the recent studied areas. The location of exposure station at each location was chosen according to local atmosphere and convenience for installations. Test period was three years, and intermittent measurements were taken three to four times during proposed exposure time.

2.1. Location of Corrosion Test Sites in Myanmar. Three exposure test sites were planned, one located in the middle of the country and the other two in the south. The location of three exposure stations is shown in Figure 1. The exposure stations are numbered as Site 1 (T1) in Mawlamyine city, Site 2 (T2) in Yangon city, and Site 3 (T3) in Mandalay city, and the corresponding numbers are used in subsequent citations. Test station T1 is located in the north-south Tenasserim (Tanintharyi) strip, test station T2 is located in the southern Irrawaddy (Ayeyarwady) deltaic cost, and test station T3 is located at the central part of the country. The major type of atmosphere in recent exposure sites is urban atmosphere. The sites are located away from the coastal line at 21 km for test station T1, 51 km for test station T2, and 342 km for test site T3, respectively. The exposure test racks were constructed according to the ISO 8565 standard [14]. The exposure racks' installations were finished on the roof slab of the universities' buildings at each site.

The climatic parameters including temperature (T) and relative humidity (RH) were recorded on an hourly basis by a meteorological observation system installed at the nearby location of test specimens. Atmospheric impurities such as airborne salt and sulfur dioxide were measured by gauze and cylinder methods according to the JIS Z 2382 standard [15]. The dry gauge and PbO_2 cylinder were installed under the instrument shelter with open airflow up to the standard. The gauge and cylinder were replaced every month, and the content of monthly atmospheric impurities was determined from the discharged gauge and cylinder. 18 flat plate specimens with a size of $70 \times 150 \times 3$ mm of

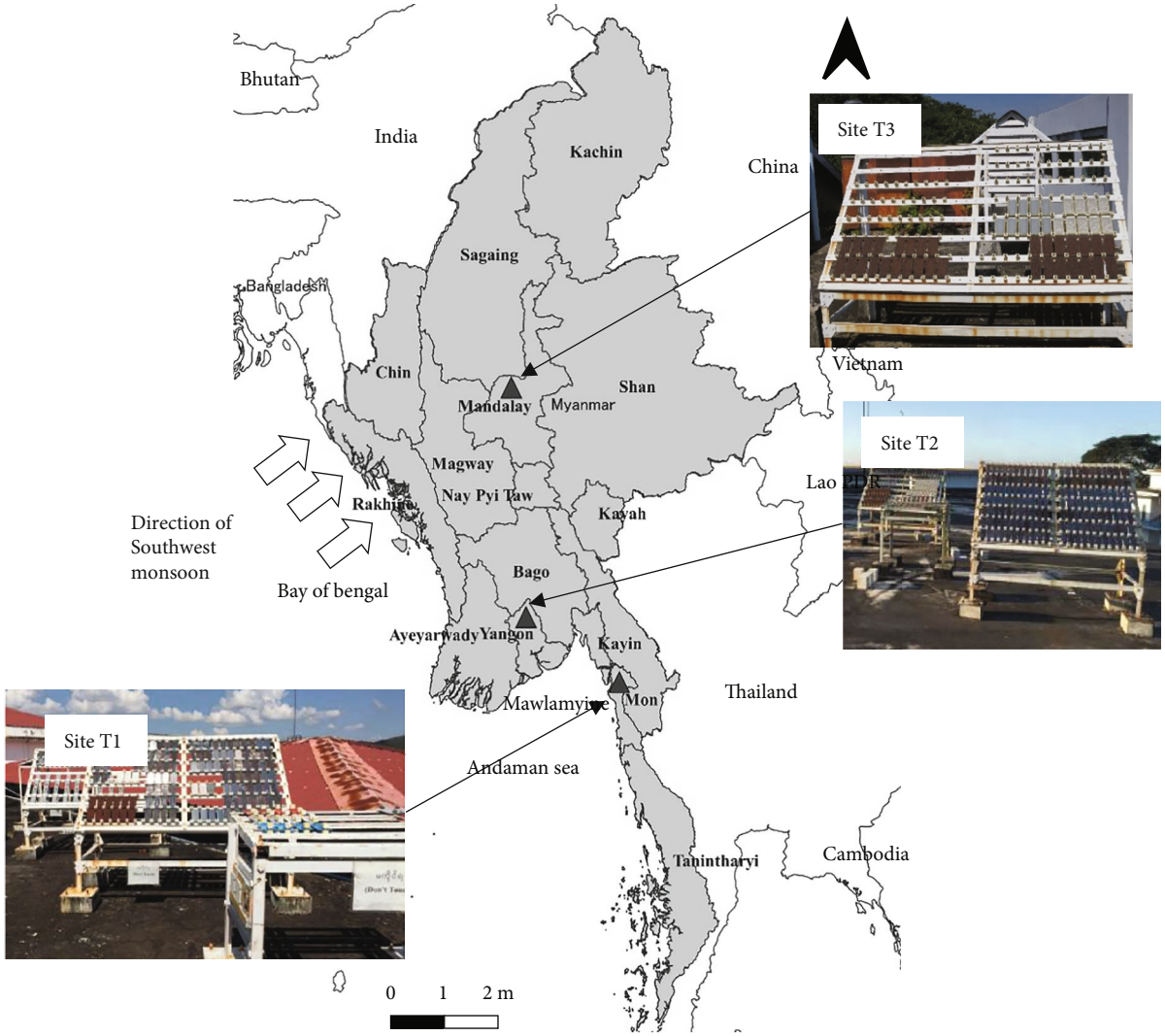

Figure 1: Locations of test sites.

carbon (SM) and weathering (SMA) steels were prepared for Sites T2 and T3, and 12 flat plate specimens were subjected to exposure at Site T1. The chemical composition of steels for this study is shown in Table 1.

The specimens were cleaned prior to the exposure at the site according to ASTM G1-03 [16]. At each exposure site, three out of the total number of specimens were dismounted at the desired sampling period. The samples were exposed at Site T1 from September 2014 to December 2014, September 2014 to April 2015, September 2014 to August 2015, and September 2014 to December 2015. At site T2, six sets of specimens were exposed from September 2014 to December 2014, September 2014 to April 2015, September 2014 to August 2015, September 2014 to December 2015, March 2014 to March 2016, and March 2014 to March 2017. Three sets of samples were taken and exposed at the test Site T3 from March 2014 to March 2015, from March 2014 to March 2016, and from March 2014 to March 2017. At the end of each sampling period, samples were collected and corrosion was investigated.

2.2. Corrosion Rate Calculation and Kinetic Studies. The amount of metallic corrosion is determined by the weight loss method in which the material's weight loss is calculated by differencing the weight of original specimens and the weight of specimens after cleaning. In this study, the specimen cleaning process is followed to the ISO 8407 standard [17]. The cleaning procedure and content of chemical solution according to the standard are shown in Table 2.

The corrosion rate calculation is carried out according to

$$\mathrm{CR(mm/yr)} = \frac{10W_y}{\rho A}, \tag{1}$$

where W_y is weight loss per year (g/y), ρ is density of steel (g/cm^3), and A is exposed area (cm^2).

To predict the mathematical model, corrosion data from 3-year exposure were used. The variation of weight loss (C) due to corrosion expressed as micrometers (μm)

Table 1: Composition of carbon steel (SM) and weathering steel (SMA).

Material	Chemical composition (% by weight)								
	C	Si	Mn	P	S	Cu	Cr	Ni	Nb
SM	0.17	0.32	1.39	0.016	0.012	—	—	—	—
SMA	0.12	0.39	0.9	0.008	0.006	0.36	0.61	0.22	0.014

Table 2: Chemical cleaning procedure and solution for removal of corrosion products.

Material	Chemical	Time	Temperature	Remarks
Iron and steel	(i) 500 ml hydrochloric acid (ii) 3.5 g hexamethylenetetramine (iii) distilled water to make 1000 ml	10 min	20 °C to 25°C	Longer time may be required in certain circumstances

with time (t) can be described by the empirical equation in the form

$$C = kt^n. \quad (2)$$

Townsend and Zoccola [18] used linear regression analysis to fit a straight line to a log-log plot of corrosion loss (C) vs. time (t) in logarithmic form:

$$\log_{10} C = \log_{10} k + n \log_{10} t, \quad (3)$$

where k is the intercept (equal to the corrosion loss in first year) and n is the slope of the log-log plot. The first year corrosion rate is important for not only the classification of atmosphere corrosivity but also for the forecasting of long-term corrosion. The value of k and n depends on type of parameter and climatic parameters. A higher n value which is greater than 0.5 suggests that the rust layer is loosely adherent and tends to result an increment in the corrosion reaction. An A value of n lower than 0.5 results from a decrease in the diffusion coefficient with time trough recrystallization, compaction of rust layer, etc.

The aggressiveness of atmosphere is classified according to the ISO 9223 standard [19]. The standard's criteria define the environmental classification in terms of SO_2 (class P) and CL^- (class S), whereas P_0, and P_1 correspond to SO_2 deposition rates of <10 and 10-35 mg m^{-2} d^{-1}, respectively, and S_0, S_1, S_2, and S_3 correspond to chloride deposition rate of <3, 3-60, 60-300, and 300-1500 mg m^{-2} d^{-1}, respectively.

2.3. Morphology of Corrosion Products. The morphology of corrosion products was analyzed using scanning electron microscopy (SEM). SEM analyses were completed using the JEOL JXA 480A Electron Probe Microanalyzer, and the samples were analyzed in the as-received condition. A SEM test was performed in the same spots on the specimen's surface.

3. Results

3.1. Time of Wetness. Myanmar is located in the tropical monsoon climate zone and has long costal line which is about 2,300 km alongside the Bay of Bangel and the Andaman Sea. Thus, the climate is strongly influenced by the monsoon and it is different from the country's South to North. According to the meteorological agency, the areas of the country are classified according to their climate characters as the coastal area, deltaic area, central dry area, and northern highland area. The country climate is classified as three seasons; the winter or northeast monsoon season (from November to February) with low temperature prevails over the whole country; the summer season (from March to the mid of May) with high temperature prevails in the central and lower parts of the country; and the rainy or southwest monsoon season (from the mid of May to October) with constantly heavy rainfall is observed in the coastal region. Monthly average climate data (temperature, T; relative humidity, RH; and rainfall) was measured by meteorological observation system installed at the exposure site.

According to measured climate data, the average temperature at all exposure sites is almost constantly high during a year, regardless of small fluctuation with less than 10°C. The maximum temperature range is within 30-35°C during the summer time (within March and May). Mandalay site (T3); located in the central dry area under temperate climate has the highest temperature among three exposure sites. As shown in Figure 2, Site T1 and Site T2 have almost the same temperature and both experience low-temperature variation during a year. Meanwhile, Mawlamyine site (T1), located in the southern region of the country, has the average temperature range of 18-29°C with a constantly high relative humidity range within 65-98% within a year. RH in Site 2 is also high, and the monthly average RH is about 58-85%. However, RH in Site 3 is obviously lower than others with a range of about 40-77%.

The total rainfall is high due to the monsoon in rainy season as can be seen in Figure 3(a). The distribution of rainfall is complicated and depends on topography. In general, the highest rainfall amount was measured in Site 1 in August, which is about 826 mm (33 inches). Meanwhile, in Site 2 (T2), the highest rainfall is about 510 mm (20 inches). The rainfall in Site 3 is very low, which is about 250 mm (10 inches) in May.

The above factors provide a calculation of the time of wetness (TOW). In this study, TOW is assumed as the time during which T is higher than 0°C and RH is greater than or

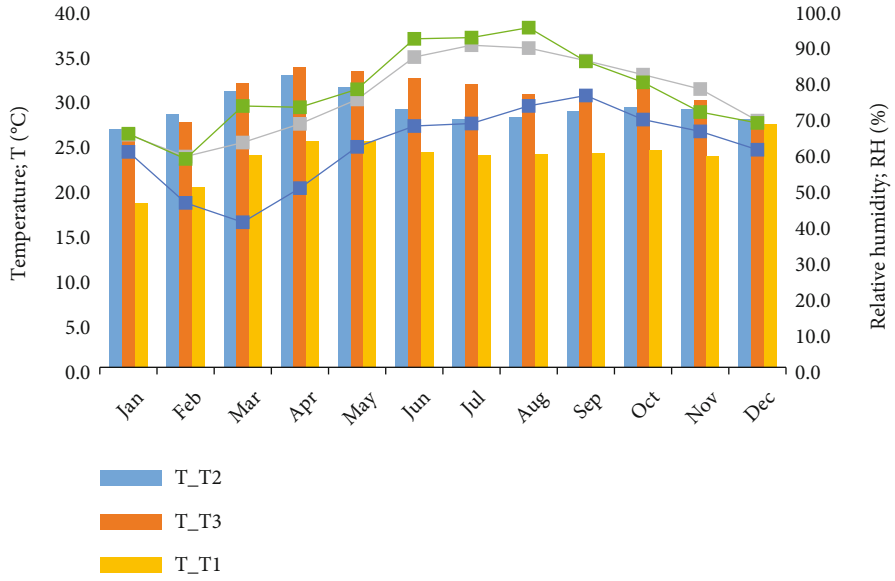

Figure 2: Temperature and relative humidity.

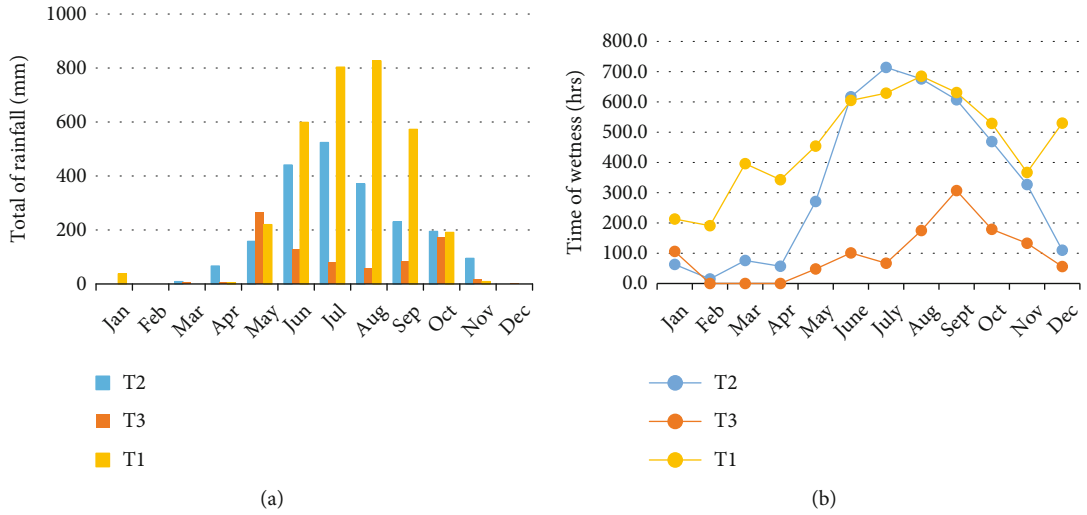

Figure 3: Total of rainfall (a) and TOW (b).

equal to 80 (%) [19]. Figure 3(b) and Table 3 give the monthly average TOW and the category of TOW of the sites. The highest monthly TOW was recorded between June and September during the rainy season. Similar to RH, TOW is high in the south; annual TOW is longest in Site 1 (T1) and is about 5532 h/year, and annual TOW in Site 2 (T2) is about 4002 h/year. In the central part, it is only a few hours which is about 1172 h/year.

According to the ISO definition of TOW, the time of wetness of the corroding surface is directly determining the duration of the electrochemical corrosion processes. However, this calculation does not cover all the aspects of climate because TOW is "estimated" based on the characteristics of the atmosphere humidity complex, independently of the pollutant level and the nature of the metallic material [20]. From this point on, it is necessary to clarify the relationship between TOW and pollution levels in the atmosphere that has combined effects on corrosion rates.

Table 3: Data of time of wetness.

Site no.	TOW (hours/year)	Category
1	5532	τ_4
2	4002	τ_4
3	1172	τ_3

3.2. Levels of Pollutants in the Atmosphere. The monthly average deposition rates of SO_2 and chloride and category of atmospheric pollutants by the ISO standard are given in Figure 4 and Table 4, respectively. It was observed that chloride deposition (about 0.06 mdd) was observed during May

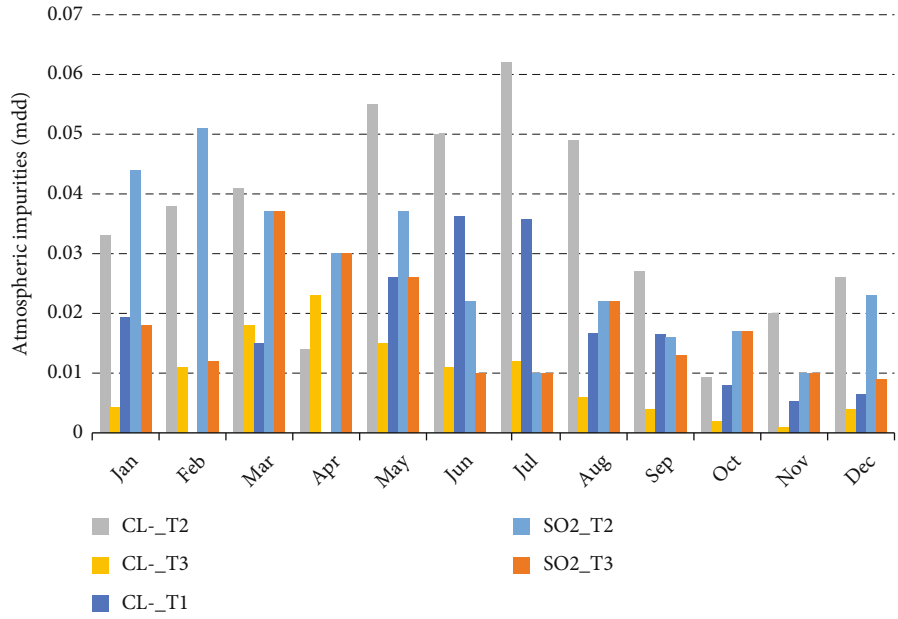

Figure 4: Atmospheric impurities at test sites.

Table 4: Average deposition rate and classification of atmospheric pollutants.

Site no.	SO_2 (mg m^{-2} day^{-1})	Deposition rate category (P)	CL^- (mg m^{-2} day^{-1})	Deposition rate category (S)
1	—	—	1.89	S_0
2	2.41	P_0	3.7	S_1
3	2.40	P_0	1.2	S_0

Table 5: Corrosion rate values and atmosphere aggressiveness.

Site no.	Specimen type	Corr. Rate (μm/year)	Category
1	SM	13.96	C2
	SMA	13.26	C2
2	SM	17.32	C2
	SMA	16.57	C2
3	SM	8.92	C2
	SMA	6.76	C2

to August (high TOW period during rainy seasons). Monsoon wind usually sweeps through the country during these times [21] causing more airborne salt particles to be carried inland by the wind. Maximum sulfur dioxide deposition measured at Site T2 was 0.05 mdd, while the rate measured at Site 3 is 0.036 mdd. The annual average values of chloride are a little higher at Site T2, the value is 3.7 mg m^{-2} day^{-1}, while at Site 1, the value is 1.89 mg m^{-2} day^{-1}. Site T3 has lesser chloride deposition rate than others which is 1.2 mg m^{-2} day^{-1}. The annual average deposition of SO_2 recorded at the sites is almost identical, 2.41 mg m^{-2} day^{-1} and 2.4 mg m^{-2} day^{-1}, at Site T2 and Site T3, respectively.

The chloride deposition in Site T1 is lower than that in Site T2 although Site T1 is closer to the coast. This is because Site T1 has higher rainfall, and it could be due to washing effect of heavy rain and carrying effect of wind on deposited atmosphere pollutants, respectively [20]. It is noted that the chloride deposition is higher during the peak TOW season, and vice versa. Here, it can be said that these two parameters have a relationship to each other. To confirm the relationship between TOW and CL^- deposition, more information is needed.

3.3. Corrosion Rates and Classification of Atmospheres Aggressiveness. The corrosivity categories of atmosphere were evaluated as defined by ISO 9223 [19]. This standard determines the corrosion rate depending on the corrosion rate of set of metals after 1-year exposure. The corrosivity category of different environments is classified under class C, wherein C1, C2, C3, C4, and C5 correspond to the corrosion rates of very low, low, medium, high, and very high, respectively. Table 5 shows the corrosion rates and corrosivity categories of the sites.

In general, both SM and SMA steels show decreased corrosion rates as the exposure time increases. All sites are classified as having low aggressive atmospheres, ISO C2 (low corrosivity).

3.4. Kinetic Studies. For the mathematical modelling relative to the corrosion rate versus time, Equation (1) is used for the atmospheric behavior of a certain material at the recent sites. Two parameters "n" and "K" define the function of corrosion of proposed materials. The initial corrosion rate (corrosion rate during the first year of exposure) is described

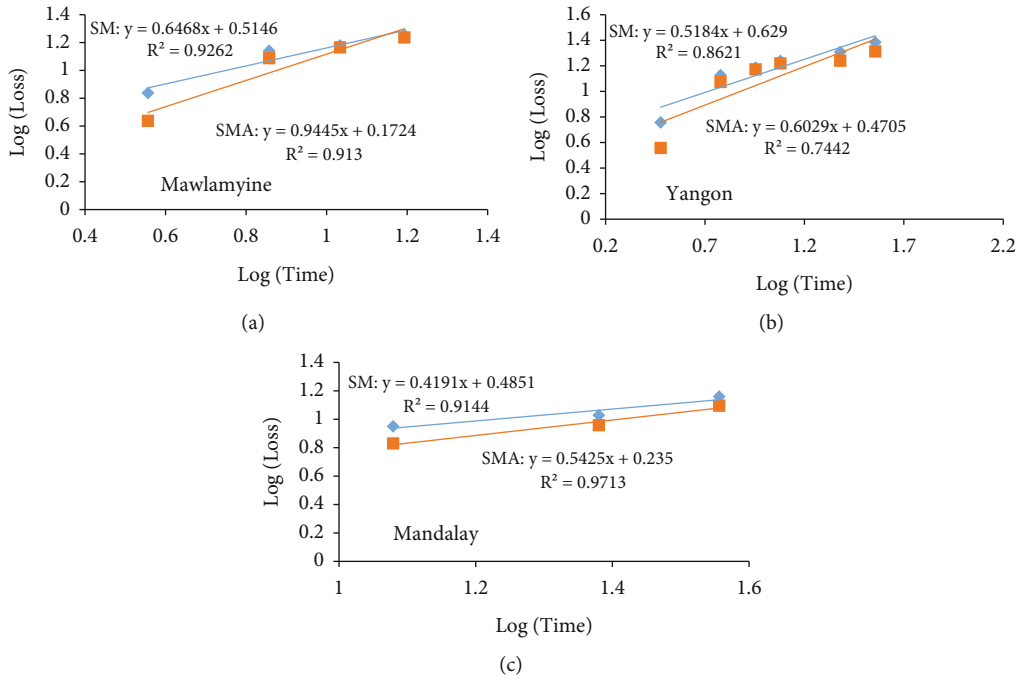

Figure 5: Logarithmic plots of corrosion loss (μm) as a function of time exposed at the sites T1 (a), T2 (b), and T3 (c).

Table 6: Corrosion kinetic parameters K, n, and coefficient of r^2.

Test station		SM			SMA		
No.	Location	K (μm)	n	r^2	K (μm)	n	r^2
T1	Mawlamyine	15.09	0.65	0.92	14.63	0.94	0.91
T2	Yangon	17.32	0.52	0.86	16.57	0.60	0.74
T3	Mandalay	8.92	0.42	0.91	6.76	0.54	0.97

by "k," while "n" is a measure of long-term decrease in corrosion rate. When $n = 0.5$, the corrosion penetration increases in parabolic, with diffusion through the corrosion product layers as the rate controlling step. At $n < 0.5$, the corrosion products show protective, passivating characteristics. A higher "n" value which is >0.5 indicates nonprotective corrosion products. As shown in Figure 5, the corrosion data versus time can be mapped to log-log coordinates to obtain an approximate point on a straight line, whose slope is taken as the "n" value.

From the figures, it can be seen that the points lie close to a straight line on the log-log coordinate. This is saying that the power function is verified to estimate corrosion behavior of steel at these three sites. The values for "n," "k," and correlation coefficient "r^2" for each site are shown in Table 6.

Nonprotective layers of rust were found in both SM and SMA due to the fact that the n values were higher than 0.5. However, the corrosion rates of SMA steels at all exposure sites are lower than those of SM steels. As a result of the alloying elements in SMA steels, corrosion rates are retarded more than conventional SM steels at all test sites where corrosion rate reduces by 2% for T1, 11% for T2, and 24% for T3.

3.5. The Observation of Corrosion Products. A composition of corrosion product depends on the material and the environment, to which it is exposed, as well as the intensity of changes in meteorological factors, such as wind, temperature, and rainfall. The scanning electron microscope (SEM) shows the morphological and topographical characteristics of the oxide layer. Throughout the period of one year of exposure, traces of oxide were found on each periodical sample. The SEM morphology of rust on carbon steel which was exposed for 12 months is illustrated in Figure 6.

The observation of corrosion product after one month of exposure (August-September) was dominantly lepidocrocite with different shapes. After two months of exposure, the corrosion products comprised of globular lepidocrocite. It was found that the corrosion products after four months (August-December) and five months (August-January) of exposure were akaganeite and magnetite. Some features, such as globular lepidocrocite, were not found on the surface of the specimens during that time. This is because of the heavy rain during the last months of rainy season (May–October) as seen in Figure 3(a) that might have cleaned the corrosion products and might be responsible for the loss of these features.

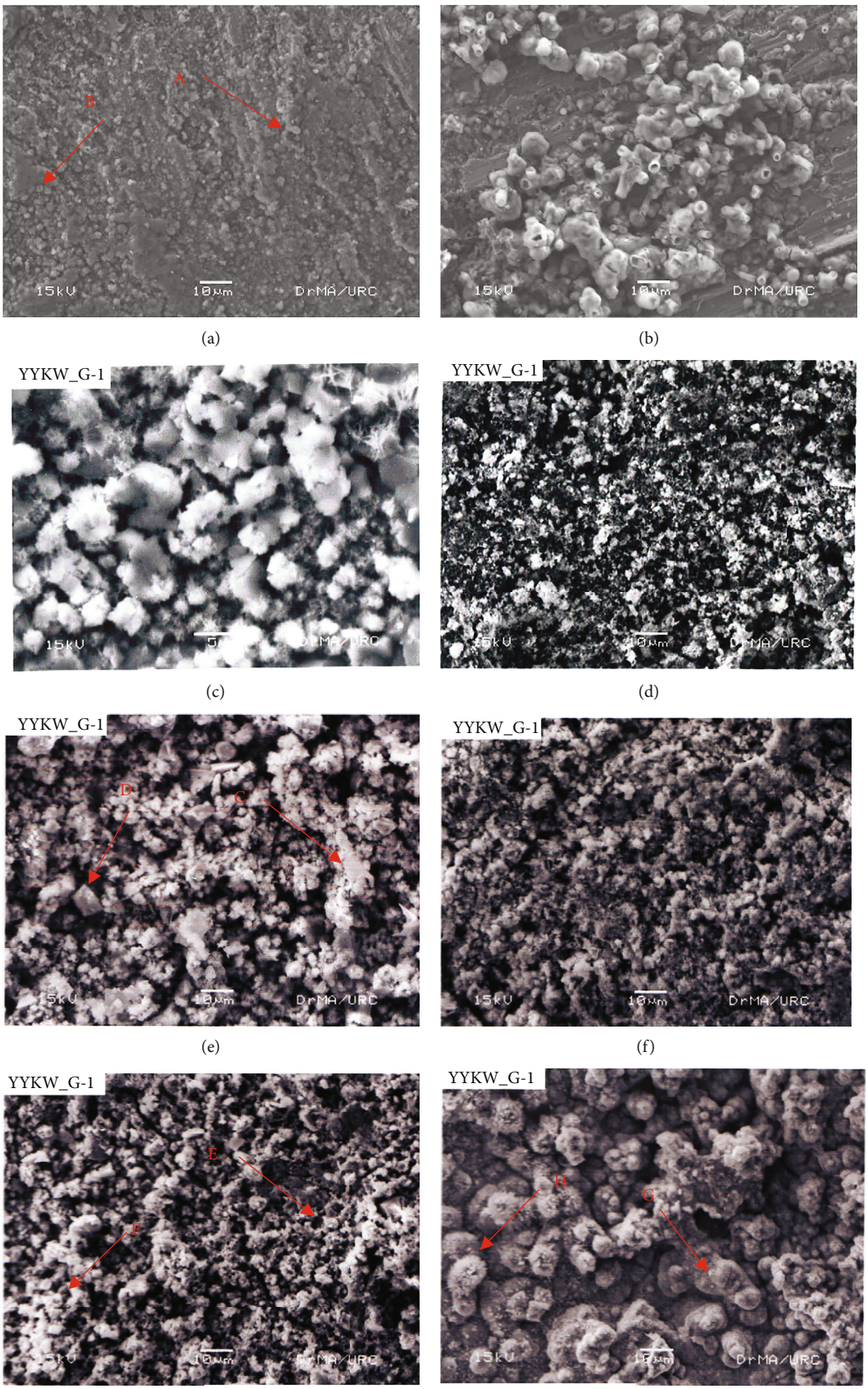

Figure 6: Continued.

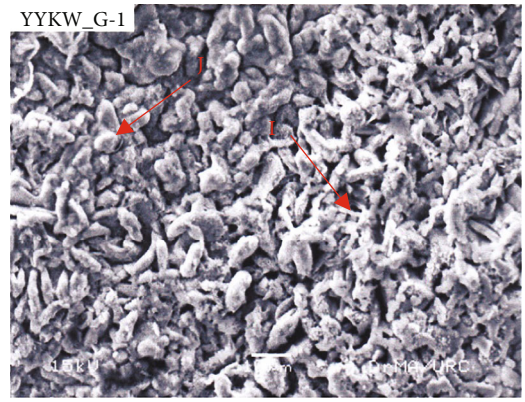

(i)

Figure 6: The morphology of corrosion products: (a) after one month: plate (A) and globular (B) lepidocrocite; (b) after two months: bar type lepidocrocite; (c) after four months: akaganeite; (d) after five months: magnetite. The morphology of corrosion products: (e) after six months: sandy crystals (C) and bar-shaped (D) lepidocrocite; (f) after seven months: sandy crystals lepidocrocite; (g) after eight months: sandy crystals (E) and flowery (F) lepidocrocite; (h) after nine months: globular (G) and needle-shaped goethite on the surface of globular (H) lepidocrocite; (i) after twelve months: worm net lepidocrocite (I) and cotton ball goethite (J).

During December to February, the amount of sulfur dioxide deposition was measured within a range of 3-5 mmd. The formation of lepidocrocite was found again in February (6 months of exposure). Lepidocrocite with different shapes such as sandy crystals and bar-shaped and flowery structures was found again after six, seven, and eight months of exposure. When the exposure time was passing, goethite emerged partly on the specimen surface. The globular and needle-shaped goethite on the globular lepidocrocite can be observed after nine-month period. The features of worm net lepidocrocite with cotton ball goethite were observed after twelve months. The early stage of weathering of carbon steel under the longer period of TOW is commonly associated with lepidocrocite. The initiation of goethite formation was started at the nine months of exposure. These features indicate the growing of goethite with the longer period of exposure.

4. Conclusions

TOW in the south part of Myanmar is high, according to ISO classification which is equivalent to class τ_4 in Site T1 and Site T2. Temperature in the central part of the country is consistently high, and TOW in Site T3 is low with an ISO class of τ_3. In Myanmar, due to the relatively low level of atmospheric impurities (such as SO_2 class, P_0 and CL^- class, S_0-S_1) and high rainfall, the corrosion rates of both SM and SMA steels highly depend on the time of wetness (TOW). The corrosion rates in both SM and SMA steels decrease with increasing exposure term. Low to medium aggressiveness of atmosphere was determined at Mawlamyine, Yangon, and Mandalay in Myanmar.

Although corrosion rates decrease with exposure time, formation of protective rust layers has not been confirmed yet on both SM and SMA steels during these 3 years of exposure. The corrosion losses of both SM and SMA steels well fitted with power model with high correlation coefficient.

In general, the corrosion products formed on carbon steel were still dominantly lepidocrocite with different shapes, and starting of goethite was growing with longer exposure term. The major morphological structures found for the corrosion products of carbon steel in Site T2 have been globular, flowery structure, sandy crystals, and worm net structures of lepidocrocite and cotton ball and needle-shaped structures of goethite. It was found that different structures of lepidocrocite formed in the early period of exposure and later, it is transforming into goethite. The transformation of lepidocrocite to goethite primarily takes place in longer TOW. The future study will be confirmed transformation of corrosion products against exposure period.

Data Availability

Data are included in the article/supplementary material/referenced in the article.

Conflicts of Interest

The authors declare that they have no conflicts of interest.

Acknowledgments

The authors offer special Thanks are due to a research group of "KUSPIRITS: Corrosion and Deterioration of Construction Materials and Strategic Maintenance of Infrastructures on Southeast Asia" for their support through the project. Special thanks are also offered to JFE Steel Corporation for their supports on test coupons. Last but not least, the authors are thankful to all who those who assisted in the research process.

References

[1] W. Thandar, K. Sugiura, Y. Kitane, and Y. Suzuki, "Atmospheric corrosion of weathering steel in Myanmar and its correlation on accelerated test," *Proceedings 10th International Conference on Bridge Maintenance, Safety and Management (IABMAS 2020)*, 2021, pp. 3872–3878, Sapporo, Japan, 2021.

[2] F. Corvo, T. Perez, L. R. Dzib et al., "Outdoor-indoor corrosion of metals in tropical coastal atmospheres," *Corrosion Science*, vol. 50, no. 1, pp. 220–230, 2008.

[3] A. Mendoza and F. Corvo, "Outdoor and indoor atmospheric corrosion of non-ferrous metals," *Corrosion Science*, vol. 42, no. 7, pp. 1123–1147, 2000.

[4] J. Morales, F. Diaz, J. Hernandez, S. Gonzales, and V. Cano, "Atmospheric corrosion in subtropical areas: statistic study of the corrosion of zinc plates exposed to several atmospheres in the province of Santa Cruz de Tenerife (Canary Islands, Spain)," *Corrosion Science*, vol. 49, no. 2, pp. 526–541, 2007.

[5] P.-A. Schweitzer, *Atmospheric Degradation and Corrosion Control*, CRC Press, United States, 1999.

[6] P. Wanida, S.-P. Namurata, K. Piya et al., "Atmospheric Corrosion monitoring sensor in corrosion rate prediction of carbon and weathering steels in Thailand," *Material Transactions*, vol. 61, no. 12, pp. 2348–2356, 2020.

[7] L.-T.-H. Lien, P.-T. San, and H.-L. Hong, "Results of studying atmospheric corrosion in Vietnam 1995-2005," *Science and Technology of Advanced Materials*, vol. 8, no. 7-8, pp. 552–558, 2007.

[8] C. Leygraf, T. E. Graedel, J. Tidblad, and I. O. Wallinder, *Atmospheric corrosion: advanced stages of corrosion*, John Wiley & Sons, New Jersey, 2016.

[9] D. De la Fuente, J. Alcántara, B. Chico, I. Díaz, J. A. Jiménez, and M. Morcillo, "Characterisation of rust surfaces formed on mild steel exposed to marine atmospheres using XRD and SEM/Micro-Raman techniques," *Corrosion Science*, vol. 110, pp. 253–264, 2016.

[10] T. Misawa, K. Hashimoto, and S. Shimodaira, "The mechanism of formation of iron oxide and oxyhydroxides in aqueous solutions at room temperature," *Corrosion science*, vol. 14, no. 2, pp. 131–149, 1974.

[11] R.-A. Antunes, I. Costa, and D. L. A. . Faria, "Characterization of corrosion products formed on steels in the first months of atmospheric exposure," *Materials Research*, vol. 6, no. 3, pp. 403–408, 2003.

[12] S. Fonna, I. Bin M Ibrahim, Gunawarman, S. Huzni, M. Ikhsan, and S. Thalib, "Investigation of corrosion products formed on the surface of carbon steel exposed in Banda Aceh's atmosphere," *Vaccine reports*, vol. 7, no. 4, 2021.

[13] T. Khaing, Y.-Y. Kyi Win, and N.-M. Kyaw, "Study on rust characterization and prediction of atmospheric corrosion rates for structural steels in Yangon (Myanmar)," *IPTEK Journal of Proceedings Series*, vol. 3, no. 6, 2017.

[14] ISO 8565, *Metals and alloys - Atmospheric corrosion testing - General requirements*, International Organization for Standardization, 2011.

[15] JIS Z 2382, *Determination of pollution for evaluation of corrosivity of atmospheres*, Japanese Standards Association, 1998.

[16] ASTM G1-03, *Standard practice for preparing, cleaning, and evaluating corrosion test specimens*, American Society for Testing and Materials, 2003.

[17] ISO 8407, *Corrosion of metals and alloys- removal of corrosion products from corrosion test specimens*, International Organization for Standardization, 1991.

[18] H.-E. Townsend and J. Zoccola, "Eight-year atmospheric corrosion performance of weathering steel in industrial, rural and marine environments," in *Atmospheric Corrosion of Metals, ASTM STP 767*, S. W. Dean Jr. and E. C. Rhea, Eds., pp. 45–49, American Society for Testing and Materials, 1982.

[19] ISO 9223, *Corrosion of metals and alloys-corrosivity of atmosphere- classification*, International Organization for Standardization, 2012.

[20] I.-T.-E. Fonseca, R. Picciochi, M.-H. Mendonca, and A.-C. Ramos, "The atmospheric corrosion of copper at two sites in Portugal: a comparative study," *Corrosion Science*, vol. 46, no. 3, pp. 547–561, 2004.

[21] L.-L. Aung, E.-E. Zin, P. Theingi et al., "Myanmar climate report," *Norwgain Meteorological Institude*, vol. 9, p. 105, 2017.